	Experiment title: **Spatially-resolved local atomic fluctuations in bulk metallic glasses**	**Experiment number**: HC-3830
Beamline: ID 11	**Date of experiment**: from: 17 October 2018 to: 22 October 2018	**Date of report**: 15.01.2020
Shifts: 15	**Local contact(s)**: Jon Wright	*Received at ESRF:*

Names and affiliations of applicants (* indicates experimentalists):

*Mihai Stoica, Metal Physics and Technology, Department of Materials, ETH Zürich, 8093 Zürich, Switzerland

*Baran Sarac, Austrian Academy of Science Erich Schmid Institute of Material Science Jahnstrasse 12, AT-8700 Leoben, Austria

*Jon Wright, ESRF, 71 avenue des Martyrs CS 40220 FR-38043 GRENOBLE Cedex 9

Report:

The proposed experiment aimed to resolve, for the first time, the local atomic fluctuation in bulk metallic glasses (BMGs). The collected X-ray diffraction (XRD) data was taken in computer tomography (CT) configuration and allowed the calculation of pair distribution function (PDF). The XRD-PDF-CT approach was used for the first time on the BMG samples, with the purpose to map their structure at nanoscale. The experiment was designed for the following glassy alloy samples: $Zr_{64.13}Cu_{15.75}Ni_{10.12}Al_{10}$, $Pt_{57.5}Cu_{14.7}Ni_{5.3}P_{22.5}$ and $Fe_{50}Ni_{30}P_{13}C_7$. Here it is worth to mention that, if the Zr- and Pt-based BMGs are known from literature, the Fe-based BMG was intensively studied by our group. Being the first time when such XRD-CT approach is applied to amorphous alloys, the method should be first validated. This is usually realized with the help of a "phantom" sample, which is artificially made by putting together few samples with different structures.

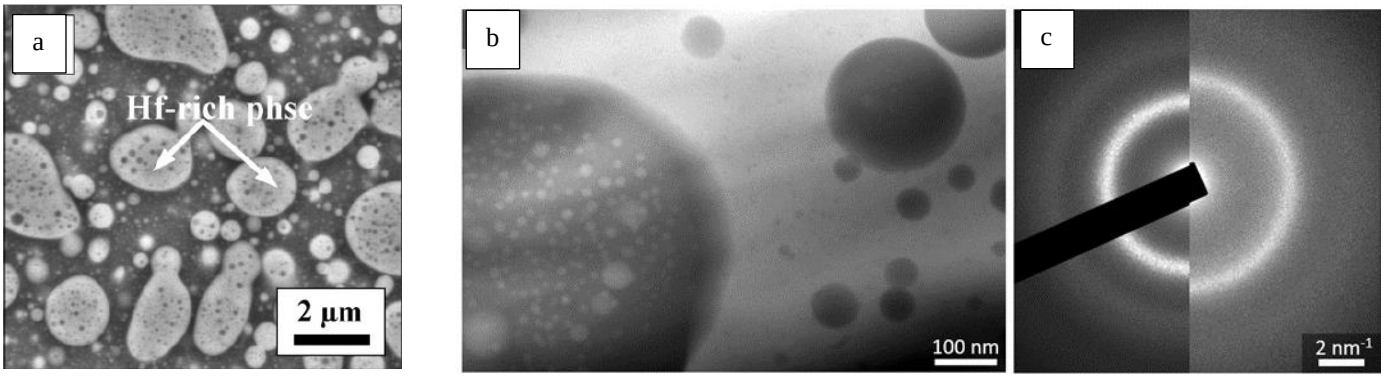

Fig. 1 Amorphous phase-separated $Gd_{27.5}Hf_{27.5}Co_{25}Al_{20}$ sample- (a) SEM image [5], (b) TEM bright-field mage, and (c) selected area diffraction pattern. The hierarhical phase separation is obvious (see the scale bar in (a) and (b)).

In order to avoid the artefacts and to have a "real" sample, we designed a hierarchical amorphous phase-separated sample (see Fig. 1) with a small volume fraction of crystalline inclusions, having the nominal composition of $Gd_{27.5}Hf_{27.5}Co_{25}Al_{20}$. The XRD-nCT was performed using a 500 nm x 500 nm focused monochromatic beam tuned at the energy of 60 keV (wave length λ = 0.020664 nm). The energy was chosen in such a way that the diffracted patterns extended over a high enough Q range and, at the same time, so that the beam could be focused to submicron dimensions. The sample, prepared as a fragment cut from a $Gd_{27.5}Hf_{27.5}Co_{25}Al_{20}$ melt-spun ribbon, was glued on a 0.5 mm diameter stiff pin and placed on a goniometer. The goniometer sat on a hexapod table which can move freely in any direction as well as rotate, with resolutions of 10 nm and 1 µrad respectively. The diffraction patterns were acquired using a 2D 2048 x 2048 pixel FReLoN detector. The scan on the Y axis extended over 100 µm, each line scan consisting of 200 points equally spaced at 0.5 µm. The scan on the ω, i.e. the rotational scan, was performed at every 1° for a total of 180°, meaning that the total number of XRD patterns was N_Y x N_ω = 36,000. Therefore the 2D resolution of the reconstructed image is 436 nm. This we may call this method **X-ray diffraction computed nanotomography (XRD-nCT)**.

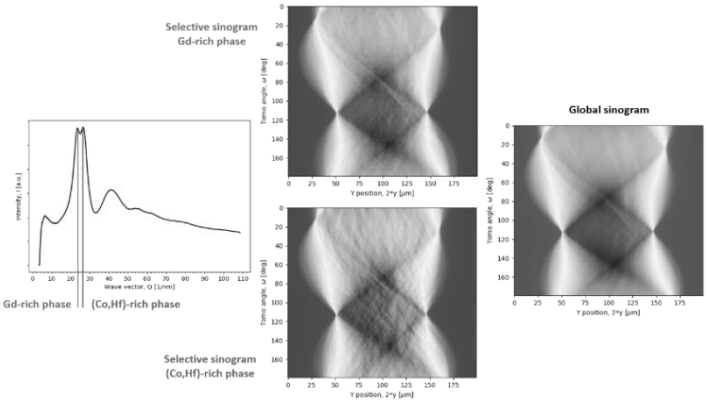

Fig. 2 Two regions of interest (ROI) corresponding to a given scattering contribution used to extract the relevant sinograms. These two regions correspond to the Gd-rich phase (lower Q value) and the Co,Hf-rich phase (higher Q value). The global sinogram, obtained by using all summed diffracted intensities, is also presented.

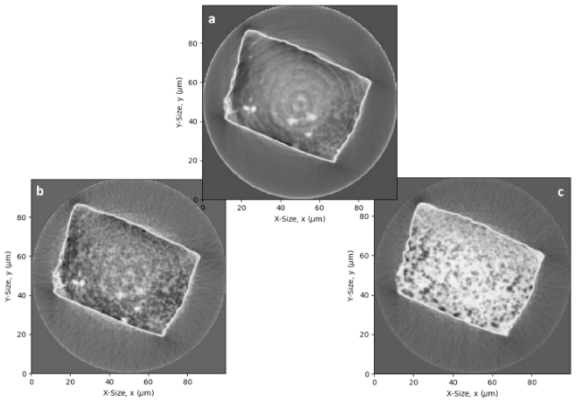

Fig. 3 The reconstructed cross-section: (a) using the global sinogram; (b) using the sinogram around the Gd-rich phase; and (c) using the sinogram around the Co,Hf-rich phase.

Fig. 2 shows the sinograms, obtained for different ROI, while Fig. 3 shows the reconstructed cross-section, using the specific sinograms. It is obvious that the strutcture is identical and even more detailed than that observed in the TEM (Fig. 1 (b)). Moreover, in order to follow a specific feature, the image can be filtered by chosing the sinogram around a specific ROI.

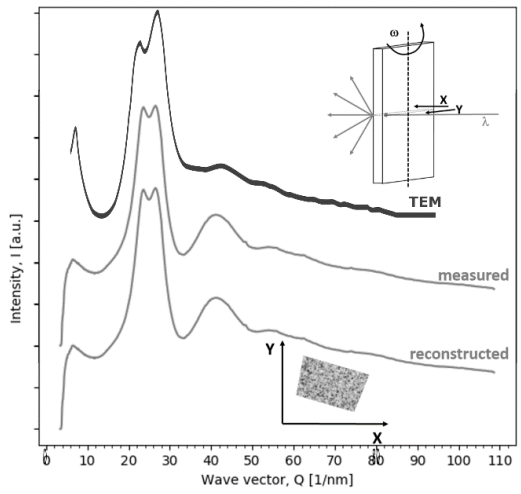

Fig. 4 Comparison of all XRD patterns.

To check whether the reconstruction was done correctly and whether it takes into account every structural detail, in Fig. 4 (left side of this text) we plotted the XRD measured and reconstructed patterns, summed up over all intensities. The actual diffracted intensity of the reconstructed XRD was normalized in order to bring all patterns in the same scale. As observed, they are identical, verifying the reliability of the reconstruction method and the entire XRD-nCT concept. Moreover, there are no differences when compared with the diffraction pattern stemming from the electron microscopy investigations.

The method was further applied to the three mentioned BMGs. The results are being evaluated and two manuscripts are on the way to be submitted.